Applied Geochemistry 63 (2015) 105–115

Contents lists available at ScienceDirect

Applied Geochemistry

journal homepage: www.elsevier.com/locate/apgeochem

Carbonate and carbon isotopic evolution of groundwater contaminated by produced water brine with hydrocarbons

Eliot A. Atekwana*, Eric J. Seeger

Boone Pickens School of Geology, 105 Noble Research Center, Oklahoma State University, Stillwater, OK 74078, USA

ARTICLE INFO

Article history:
Received 22 March 2015
Received in revised form
30 July 2015
Accepted 1 August 2015
Available online 5 August 2015

Keywords:
Produced water brine
Dissolved inorganic carbon
Stable carbon isotopes
Carbonate evolution

ABSTRACT

The major ionic and dissolved inorganic carbon (DIC) concentrations and the stable carbon isotope composition of DIC ($\delta^{13}C_{DIC}$) were measured in a freshwater aquifer contaminated by produced water brine with petroleum hydrocarbons. Our aim was to determine the effects of produced water brine contamination on the carbonate evolution of groundwater. The groundwater was characterized by three distinct anion facies: HCO_3^--rich, SO_4^{2-}-rich and Cl^--rich. The HCO_3^--rich groundwater is undergoing closed system carbonate evolution from soil $CO_{2(g)}$ and weathering of aquifer carbonates. The SO_4^{2-}-rich groundwater evolves from gypsum induced dedolomitization and pyrite oxidation. The Cl^--rich groundwater is contaminated by produced water brine and undergoes common ion induced carbonate precipitation. The $\delta^{13}C_{DIC}$ of the HCO_3^--rich groundwater was controlled by nearly equal contribution of carbon from soil $CO_{2(g)}$ and the aquifer carbonates, such that the $\delta^{13}C$ of carbon added to the groundwater was −11.6‰. In the SO_4^{2-}-rich groundwater, gypsum induced dedolomitization increased the ^{13}C such that the $\delta^{13}C$ of carbon added to the groundwater was −9.4‰. In the produced water brine contaminated Cl^--rich groundwater, common ion induced precipitation of calcite depleted the ^{13}C such that the $\delta^{13}C$ of carbon added to the groundwater was −12.7‰. The results of this study demonstrate that produced water brine contamination of fresh groundwater in carbonate aquifers alters the carbonate and carbon isotopic evolution.

1. Introduction

Produced water brine containing petroleum hydrocarbons from oil field operations are a major source of groundwater contamination at thousands of sites across the USA and the world (e.g., Kharaka and Otton, 2007; Otton et al., 2007). Produced water brine is an environmental contaminant and investigations of produced water brine contaminated sites focus on defining the spatial extent of contaminant plumes, the magnitude of contamination and the short to long term attenuation of the contamination from major ion chemistry (e.g., Herkelrath et al., 2007; Kharaka et al., 2007; Whittemore, 2007).

Many studies that have investigated the effects of the chemical and biological degradation of petroleum products (e.g., jet fuel or diesel) on carbonate evolution in fresh groundwater have used concentrations of dissolved inorganic carbon (DIC) and stable carbon isotopes ($\delta^{13}C$) of DIC (e.g., Fang et al., 2000; Godsy et al., 2003; Atekwana et al., 2005; Scow and Hicks, 2005; Whittemore, 2007; Parker et al., 2012). Recently, Su et al. (2013) investigated a site contaminated by hydrocarbons from oil field activities. However, produced water brine was not an important component of the contaminants at the site. Most studies investigating highly saline water contamination are focused on salt-water intrusion in coastal aquifers where hydrocarbon contamination is usually not a concern (e.g., Cates et al., 1996; Nicholson and Fathepure, 2005; Ulrich et al., 2009; Currell and Cartwright, 2011). The produced water brine and the chemical and biological degradation of petroleum hydrocarbons are likely to have a significant impact on the carbonate evolution of contaminated fresh groundwater.

The carbonate evolution of fresh groundwater can be determined from equilibrium and mass balance approaches based on weathering of watershed and aquifer rocks (Drever, 1997). Data on the chemical reactions and their effects on carbonate evolution occurring in fresh groundwater contaminated by produced water brine with hydrocarbons are lacking. In this study we investigate carbonate reactions in fresh groundwater that was contaminated by produced water brine with hydrocarbons. We aim to develop an understanding of the carbonate evolution in a freshwater aquifer contaminated by produced water brine. Our objectives were to (1)

* Corresponding author.
E-mail address: eliot.atekwana@okstate.edu (E.A. Atekwana).

http://dx.doi.org/10.1016/j.apgeochem.2015.08.001
0883-2927/

document the spatial and temporal chemical and stable carbon isotopic characteristics of fresh groundwater contaminated by produced water brine and (2) determine the effect the contamination and subsequent reactions on the carbonate evolution.

2. Study site

2.1. Site history

The study site is located at an abandoned oil production site in Skiatook, Oklahoma, USA (Fig. 1). The study site (site A) is one of two sites in Oklahoma previously investigated by the US Geological Survey (USGS) under the Osage-Skiatook Petroleum Environmental Research (OSPER) project. Between the mid 1910's to the late 1970's, about 100,000 barrels of oil was extracted and the produced water brine associated with the operation was stored in unlined, earthen pits on site (Kharaka et al., 2005). The produced water brine was discharged into an ephemeral creek to the north of the site creating a salt scar (Kharaka et al., 2005; Otton et al., 2007). The salt scar, with erosion up to 2 m below the surface, extends from the pre-1937 pits to the lakeshore of the NE cove of Skiatook Lake (Fig. 1). Skiatook Lake was constructed in 1987, creating a peninsula at the study site. The USGS identified the produced water brine at the study site to be a Na–Ca–Cl brine with a salinity of ~150,000 mg/L total dissolved solids, and high concentrations of Mg^{2+}, Sr^{2+} and NH_4^+ and low concentrations of SO_4^{2-} and H_2S (Kharaka and Otton, 2003). Over time, the produced water brine stored in the earthen pits seeped into the fresh groundwater creating a high salinity hydrocarbon plume (Herkelrath et al., 2007).

2.2. Geology

The study site is nested in a saddle between two hills, with a drainage divide running generally NW–SE through the middle of the site (Fig. 1). Detailed geology of the study site is reported by Otton et al. (2007) and is briefly summarized below. Five units identified from surface mapping and coring are shown in the schematic cross section (Fig. 2) along profile A–A′ shown in Fig. 1. The surficial sediments consist of unconsolidated very fine grain eolian sands and colluvium in a sandy to clayey matrix. Unit 1, which is a weathered sandstone is of limited areal distribution and only found in the northwest portion of the site. Unit 2 occurs throughout the site and consists of weathered, very fine-grained sandstone and clayey sandstone cemented by Fe oxyhydroxide. Unit 3 intertongues with Unit 2 and consists mostly of weathered shale, sandy siltstone, sandy mudstone and sandstone which is exposed within the salt scar. The unweathered shale contains abundant pyrite and gypsum. Unit 4 consists of dolomite cemented unweathered sandstone, clay partings and thin shale beds that are carbonaceous and have fossil detritus. Unit 5 contains interbedded muddy sandstone, shale, siltstone and mudstone, with the sandstone cemented by dolomite.

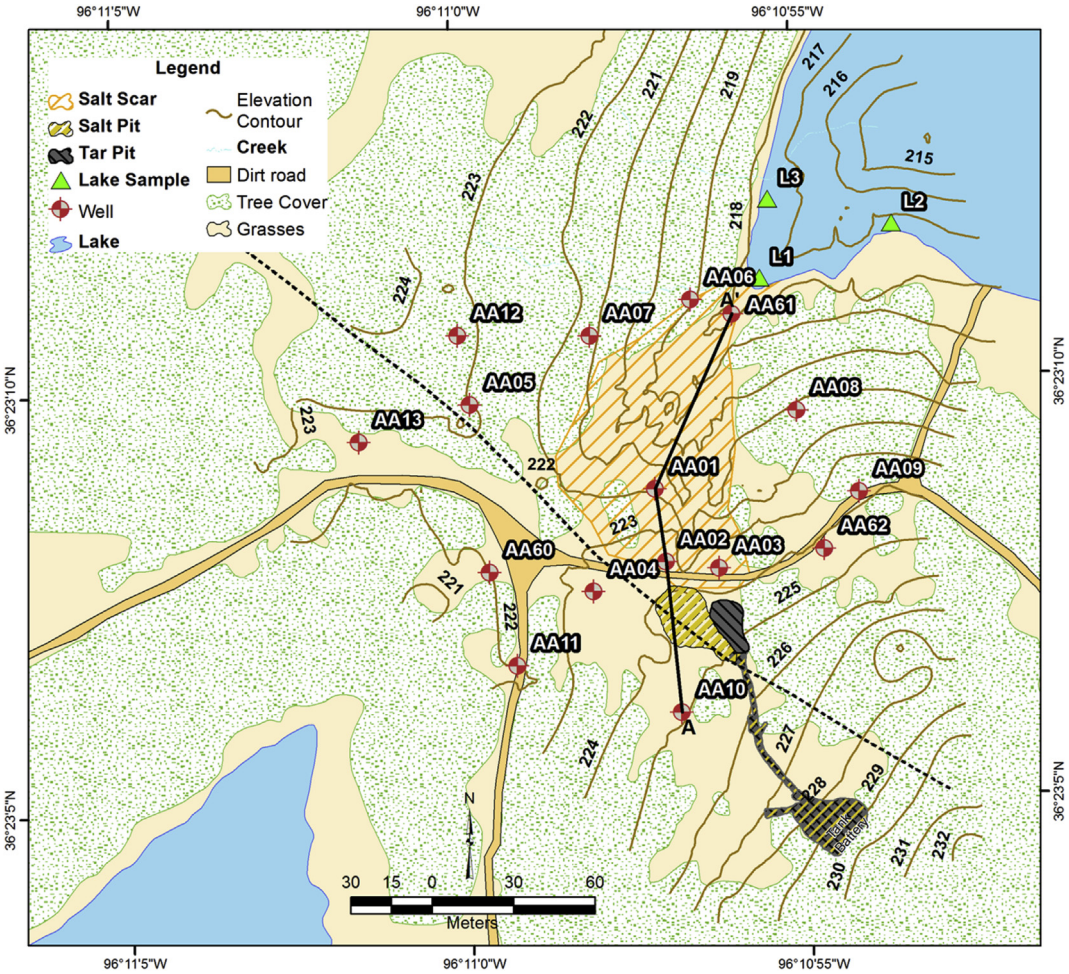

Fig. 1. Map of study site (Site A at Skiatook Lake, Osage County), Oklahoma, USA showing monitoring well locations, salt scar, oil and salt pits and transect A–A′. The dash line depicts the drainage divide at the study site.

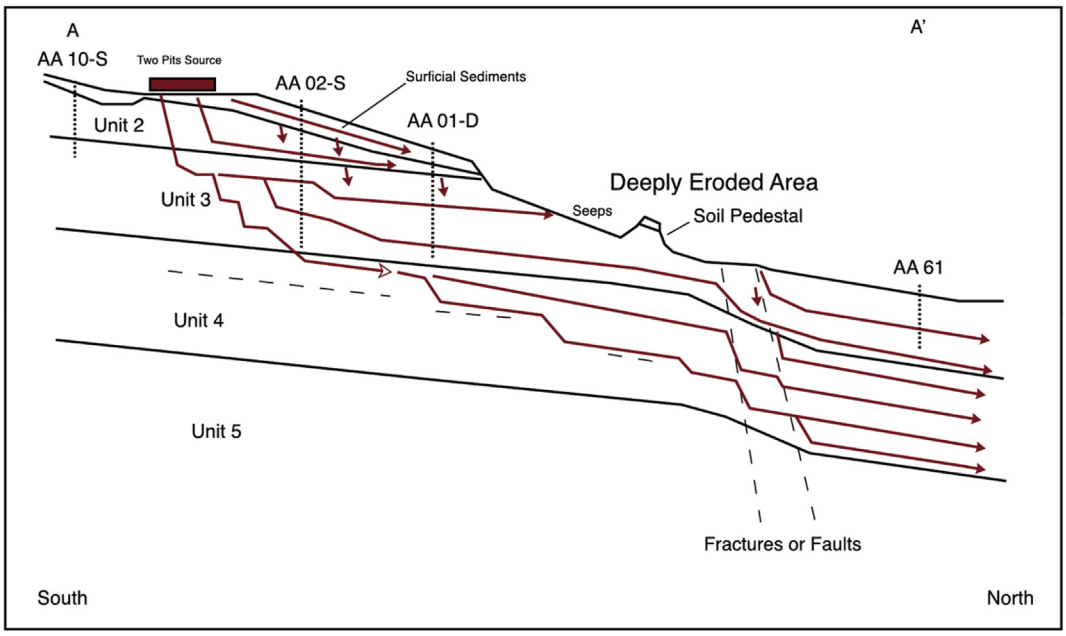

Fig. 2. Conceptual schematic of geologic units along transect A–A′ showing likely groundwater flow paths. Refer to Fig. 1 for transect location. Modified from Otton et al. (2007).

A structural lineament extends across the site along a topographic low trending N45°E from the southwest cove to the northeast cove. Vertical and subvertical fractures and faults are common and have slickensided surfaces and juxtaposed lithologies (Fig. 2). Vertical movement along the faults is estimated to be less than 1 m. Several NE-trending fault segments were mapped in the area surrounding the study site by Gardner (1957).

2.3. Hydrology

The study site is in a temperate semi-arid climate. The average annual precipitation in the region is 89 cm and the annual potential evapotranspiration is estimated at 180 cm (Herkelrath et al., 2007). The drainage divide extending NW–SE across the study site directs surface water flow to one of two coves (Fig. 1). Surface runoff north of the divide near the tar and salt pits flows NW and then turns NE to discharge into the north cove. Surface runoff south of the divide flows SSW and then turns to the SW to discharge into the SW cove.

Depth to groundwater varies at the site because of variations in topography. Groundwater flows to the NW following the dip of the bedrock, along bedding planes and penetrating deeper through the units via the fractures and faults (Fig. 2). The aquifer has an average recharge rate of about 1 cm/a (Herkelrath et al., 2007). The hydraulic conductivity of the aquifer ranges from 0.3 to 7.0 cm/d and averages 1.9 cm/d (Herkelrath et al., 2007). The sandstone aquifer units (units 1–5) are confined and not well connected to the soil zone and surface except where the salt scar exist and all soil has been removed (Herkelrath et al., 2007). Groundwater levels do not respond to individual rainfall events, however, there is a seasonal variation reflecting seasonal rainfall patterns (Herkelrath et al., 2007). Groundwater is recharged from January to June and groundwater level declines from July to December.

3. Methods

3.1. Sample collection

3.1.1. Groundwater

As part of the OSPER project, the USGS installed 34 monitoring wells, distributed inside and outside the visible salt scar (Fig. 1). Each sampling location has two monitoring wells drilled to different depths: shallow (s) and deep (d), except locations AA10 and AA11 which have three depths; shallow (s), medium (m), and deep (d). The well depths range from 1.22 to 23.46 m.

Sampling for groundwater was conducted seasonally in October 2008, February 2009, June 2009 and May 2010. Prior to making physical measurements and collecting groundwater samples, depth to groundwater in each monitoring well was measured with an electronic water-level tape. Following this, the monitoring wells were purged using either a peristaltic pump or a submersible pump. During purging, the specific conductance (SPC) and pH were monitored using a calibrated (according the manufacturers recommendations) Yellow Spring Instruments (YSI) multi-parameter probe until the readings were stable, indicating flow of formation water into the well bore. After the SPC and pH were stable, the total dissolved solids (TDS), dissolved oxygen (DO) and pH were recorded from the YSI probe.

All water samples were filtered through 0.45 μM pore size nylon syringe filters before collection. Samples for major cation analysis were collected in 60 mL polypropylene bottles and acidified to a pH < 2 with high purity nitric acid. Samples for major anion analysis were collected unacidified in 30 mL polypropylene bottles. Samples for benzene, toluene, ethylbenzene and xylenes (BTEX) analysis were collected during the May 2010 sampling event and stored in 30 mL glass vials pre-acidified with hydrochloric acid. Samples to measure DIC concentrations and $\delta^{13}C_{DIC}$ were collected in pre-evacuated vacutainers containing magnets and 1 mL of phosphoric acid as described by Atekwana and Krishnamurthy (1998). All the samples were cooled on ice and transported to the laboratory where they were stored at 4 °C until analysis.

3.1.2. Lake water

Lake water samples were collected from the north cove of Skiatook Lake along the shore at three locations (Fig. 1). The TDS, DO and pH were recorded using the YSI probe immersed into lake water. Water was collected by the grab technique using a 1 L polypropylene bottle attached to the end of a telescoping pole approximately 3 m from the lake's edge. Aliquots were collected for

various analyses and preserved as described above.

3.1.3. Tar and salt pits

The leachate from the asphaltic material in the tar pit was collected by squeezing water from the material into 50 mL centrifuge tubes that were taken to the laboratory and filtered through 0.45 μM filters using a vacuum pump. Aliquots of samples were collected for cations and anions. To collect samples to measure DIC concentrations and $\delta^{13}C_{DIC}$, we created a small depression in the tar material and allowed water to drain into it. We used a 10 mL syringe to withdraw the water which was filtered directly into the pre-evacuated acidified vacutainers. The physical parameters for water pooled in the tar and salt pits (Fig. 1) were measured once in June 2009 after 4.11 cm of rainfall which fell over seven days. The physical parameters were measured by immersing the YSI probe into the pooled water. Samples of pooled water for chemical analyses were collected by the grab technique, filtered and stored in polypropylene bottles as described for groundwater.

3.2. Sample analyses

Alkalinity was determined by acid titration immediately after filtration in the field (Hach Company, 1992). Major anions (Cl^- and SO_4^{2-}) were measured by ion chromatography and major cations (Na^+, Mg^{2+} and Ca^{2+}) were analyzed by ion chromatography and inductively coupled plasma-optical emission spectrometry. Analysis of samples for BTEX was performed by Ecological Research and Management Incorporated Environmental Laboratories, Dallas, Texas USA.

DIC concentrations were determined by extraction and cryogenic purification of $CO_{2(g)}$ using a vacuum line and the extracted $CO_{2(g)}$ was stored in 6 mm Pyrex tubes (Atekwana and Krishnamurthy, 1998). The stable carbon isotope composition of the $CO_{2(g)}$ was measured using a Thermo Finnigan Delta plus XL isotope ratio mass spectrometer. Stable carbon isotope ratios are reported in the delta (δ) notation in per mil (‰):

$$\delta(‰) = \left(\left(R_{sample} / R_{standard}\right) - 1\right) \times 1000$$

where R is $^{13}C/^{12}C$. The δ values for the carbon isotopes are reported relative to the Vienna Pee Dee Belemnite standard. Routine isotopic measurements of in-house standards and samples have an overall precision ($1 - \sigma$ standard deviation) of better than 0.1‰.

3.3. Determination of water types and mineral saturation indices

The results of the sample analyses were uploaded to AquaChem (Calmbach, 1997) where water types were determined and plotted on a piper diagram. PhreeqcI version 2 was used to calculate the saturation indices with respect to calcite and dolomite and the partial pressure of CO_2 (pCO_2) using the temperature, pH and DIC concentrations (Parkhurst and Appelo, 1999).

4. Results

4.1. TDS, DO and pH

The TDS, DO and pH results are presented in Table S1 (Supporting material). The average TDS concentration for the groundwater samples was 6110 ± 5154 mg/L and TDS concentrations ranged from 632 mg/L to 18,800 mg/L. The TDS concentrations for lake samples ranged from 137 to 176 mg/L and averaged 149 ± 15 mg/L. The TDS concentrations for leachate in the tar pit ranged from 4820 to 118,000 mg/L and averaged 44,200 ± 54,100 mg/L. The TDS concentration was 35 mg/L for water pooled in the salt pit. The DO concentrations in groundwater averaged 2.7 ± 2.1 mg/L and ranged from 0.3 to 9.5 mg/L and was 6.4 mg/L in the salt pit. For lake samples, the DO concentrations averaged 10.0 ± 3.3 mg/L and ranged from 6.9 to 16.6 mg/L. The DO concentration in water pooled in the tar pit was 1.8 mg/L. The pH of groundwater ranged from 4.5 to 7.6 and averaged 6.1 ± 0.8. The pH of lake samples ranged from 6.0 to 8.8 and averaged 7.8 ± 0.8. Water pooled in the tar pit had a pH value of 6.5 and was 7.9 in the salt pit.

4.2. Alkalinity, Cl^- and SO_4^{2-}

The alkalinity, Cl^- and SO_4^{2-} results are presented in Table S1 (Supporting material). The alkalinity (as $CaCO_3$) concentrations in groundwater ranged from less than 1–618 mg/L and averaged 227 ± 144 mg/L. Lake samples had alkalinity concentrations that ranged from 27 to 96 mg/L and averaged 59 ± 16 mg/L. Alkalinity in water pooled in the tar pit was 17 mg/L and <1 mg/L in water pooled in the salt pit. The Cl^- concentrations in groundwater ranged from 36 to 10,500 mg/L and averaged 2920 ± 2870 mg/L. The Cl^- concentrations for lake samples averaged 23 ± 3 mg/L and ranged from 19 to 28 mg/L. The averaged Cl^- concentration for leachate in the tar pit was 31,200 mg/L and ranged from 1080 to 64,700 mg/L and the Cl^- concentration of water pooled in the salt pit was 5 mg/L. For the groundwater samples, the averaged SO_4^{2-} concentration was 339 ± 384 mg/L with a range from 1 to 1270 mg/L. Lake samples had an averaged SO_4^{2-} concentration of 10 ± 2 mg/L which ranged between 7 and 13 mg/L. Leachate in the tar pit had an averaged SO_4^{2-} concentration of 44 ± 6 mg/L which ranged from 38 to 53 mg/L and water pooled in the salt pit had a SO_4^{2-} concentration of 3 mg/L.

4.3. Na^+, Ca^{2+} and Mg^{2+}

The Na^+, Ca^{2+} and Mg^{2+} results are presented in Table S1 (Supporting material). The Na^+ concentrations averaged 1090 ± 942 mg/L in the groundwater samples and ranged from 75 to 3450 mg/L. The averaged concentrations of Na^+ in the lake samples was 12 ± 4 mg/L and the concentrations ranged between 6 and 18 mg/L. Leachate in the tar pit had an averaged concentration of Na^+ of 17,100 ± 13,400 mg/L with a concentration range of 743–33,500 mg/L and water pooled in the salt pit was 2 mg/L. The averaged concentration of Ca^{2+} for groundwater was 496 ± 531 with a concentration range between 20 and 2620 mg/L. The averaged concentration for Mg^{2+} for groundwater samples was 341 ± 418 mg/L with a concentration range between 5 and 1860 mg/L. In the lake samples, Ca^{2+} concentrations ranged from 20 to 26 mg/L and averaged 23 ± 2 mg/L, while Mg^{2+} concentrations ranged from 2 to 7 mg/L and averaged 5 ± 1 mg/L. Leachate in the tar pit had a Ca^{2+} concentration range between 156 and 5940 mg/L with an average of 3050 ± 2360 mg/L, while Mg^{2+} concentrations ranged between 95 and 1620 mg/L and averaged 806 ± 625 mg/L. Water pooled in the salt pit had a Ca^{2+} concentration of 2 mg/L and the Mg^{2+} concentration was below detection.

4.4. Benzene, toluene, ethylbenzene and xylenes (BTEX)

The results for analyses for benzene, toluene, ethylbenzene and xylenes (BTEX) in groundwater and the lake samples were all below detection limit (<2.0×10^{-4} mg/L).

4.5. DIC and $\delta^{13}C_{DIC}$

The DIC and $\delta^{13}C_{DIC}$ results are presented in Table S1 (Supporting material). The DIC concentrations for groundwater averaged

68 ± 31 mg C/L and ranged between 8 and 194 mg C/L. DIC concentrations in lake samples averaged 11 ± 2 mg C/L and ranged from 6 to 14 mg C/L. The $\delta^{13}C_{DIC}$ of groundwater averaged −15.3‰ ± 3.7‰ and ranged from −8.6 to −23.5‰. The $\delta^{13}C_{DIC}$ of lake samples averaged −7.7‰ ± 1.4‰ and ranged from −5.4 to −9.1‰. The concentration of DIC of water collected from the tar pit in February 2009 was 37 mg C/L and the $\delta^{13}C_{DIC}$ was 5.9‰, while the sample collected in May 2010 had a DIC concentration of 82 mg C/L and a $\delta^{13}C_{DIC}$ of 10.7‰.

4.6. Spatial and seasonal distribution of physical, chemical and isotopic parameters

Transect A–A′ (Fig. 1) is used to display the spatial variation of select physical, chemical, and isotopic results with respect to the salt scar. Transect A–A′ begins south of the pits (monitoring well AA10), crosses the drainage divide and the pits, and follows the general groundwater flow direction, ending at the edge of the lake on the north side of the study site (monitoring well AA61).

The spatial variations in TDS, Cl^-, pH, DO, SO_4^{2-}, Ca^{2+}, Na^+, alkalinity, DIC and $\delta^{13}C_{DIC}$ are shown for October 2008, February 2009, June 2009 and May 2010. It is clear from the plots that the concentration of the parameters south of the drainage divide are generally lower and less variable compared to the north portion of the site (Fig. 3). North of the drainage divide, variations at each location are due to seasons. For example, the variations in the concentration of TDS and Cl^- (a conservative tracer) appear to be related to seasonal precipitation recharge, with lower concentrations during the spring from snow recharge and in the summer from rain recharge and the higher concentrations in the fall and winter occur from limited precipitation recharge. Groundwater had lower concentrations for TDS and Cl^- in June 2009 and May 2010 and higher concentrations in October 2008 and February 2009 (Fig. 3). The pH increased from ~5.5 near the drainage divide northwards to ~7.0 near the lake. The DO and Na^+ concentration are depressed and the SO_4^{2-}, Ca^{2+} and alkalinity concentrations are highly elevated relative to the upgradient and downgradient monitoring wells (Fig. 3).

For all the sampling events, the DIC concentrations south of the drainage divide was relatively consistent at about 50 mg C/L (Fig. 3). Across the drainage divide, the DIC concentrations generally decrease from the pits northward toward the lake. The $\delta^{13}C_{DIC}$ values range from −16.0 to −21.0‰ south of the drainage divide, and north of the divide, $\delta^{13}C_{DIC}$ values increase from monitoring well AA02 near the drainage divide towards the lake to monitoring well AA61 (Fig. 3). This increase in the $\delta^{13}C_{DIC}$ values is concomitant with the decrease in DIC concentrations along the groundwater flow path.

5. Discussion

5.1. Extent of produce water brine contamination of fresh groundwater

The USGS identified the produced water brine at the study site to be a Na–Ca–Cl brine with high concentrations of Mg^{2+}, Sr^{2+} and NH_4^+ and low concentrations of SO_4^{2-} and H_2S (Kharaka and Otton, 2003). The USGS sampled groundwater in two wells (Bolin Well and Hum Well) near the study site that were considered to be uncontaminated. The Cl^- concentrations ranged from 24 to 216 mg/L. Since Cl^- has been shown to be a conservative ion at the study site (Kharaka and Otton, 2003), Cl^- is used to distinguish the degree to which the fresh groundwater is contaminated. The extent of produced water brine contamination at the site varies spatially in a radial pattern from the pit source depending on the distance from the source and seasonal fresh water recharge from precipitation. There is a positive relationship between TDS and Cl^- for groundwater contaminated by produced water brine (Fig. 4). The samples from the tar pit define this trend at higher TDS-Cl^- concentrations (Fig. 4). The highest Cl^- concentrations are found centrally at the site, directly along the main groundwater flow path from the pit source towards the lake cove to the north (Fig. 3).

We also observe that the degree to which fresh groundwater is contaminated by produced water brine has decreased over time. When we compared our results to those collected by the USGS in 2002–2005, the maximum TDS of 20,000 mg/L represents a 30% decrease over the intervening 5 y period. Although the overall concentration of the contaminants has decreased from the time the USGS first sampled groundwater in 2002 to the time of the last sampling during this study in 2010 (Fig. 4), only monitoring wells with the highest TDS concentrations (AA01-D, AA07-S, AA07-D and AA06-S) show markedly decreased TDS concentrations. The Cl^- in the tar pit was 64,700 mg/L and in the salt pit was 5 mg/L. Because of the significantly low concentration of Cl^- in the salt pit, the tar pit is a source of salt to the fresh groundwater. South of the drainage divide, groundwater at some locations have Cl^- concentrations higher than background groundwater, indicating produced water brine contamination. Southwest of the pits and south of the drainage divide is an old trench that was used to transport the oil and produced water brine to the pits (Fig. 1). Residual oil and produced water brine from the trench is likely the source of contamination of groundwater south of the drainage divide.

5.2. Chemical evolution of fresh groundwater contaminated by produced water brine

5.2.1. Major ionic proportions

The relative proportion of cations and anions (Fig. 5) can be used to infer water–rock interaction and chemical evolution of groundwater (e.g., Drever, 1997). The groundwater samples show cation proportions that vary in Ca^{2+} by 90%, in Mg^{2+} by 60% and in $Na^+ + K^+$ by 90%. In contrast, the groundwater samples cluster in three anion groupings: Cl^--rich (60–98%), SO_4^{2-}-rich (90–98%) and HCO_3^--rich (50–70%). All water samples that have Cl^- concentrations within the range of the Bolin and Hum background groundwater (24–216 mg/L) have either HCO_3^- or SO_4^{2-} as their dominant anion. Whereas, the chemical facies of the groundwater with Cl^- concentrations greater than the Bolin and Hum background groundwater change from a Na–Cl water type (e.g., AA02-S; Table S1 (Supporting material)) to a mixed-cation-Cl water type (e.g., AA61; Table S1 (Supporting material)) along the groundwater flow path from the pit source towards the north into the lake. This suggests that the concentrations of cations and anions cannot be solely attributed to produced water brine mixing with fresh groundwater. The chemical evolution of groundwater at the study site can be attributed to produced water brine mixing with fresh groundwater, water–rock interactions involving the dissolution and precipitation of minerals, microbial degradation of organic material and biodegradation of hydrocarbon mixed with the produced water brine.

The high Cl^- concentrations in the groundwater at the study site are the result of produced water brine contamination. Groundwater collected from monitoring well AA13 (shallow and deep) has low concentrations of TDS and Cl^- and can be considered as background groundwater. As the produced water brine contamination migrates through the aquifer, we anticipate that Cl^- concentrations will maintain a nearly constant ratio to TDS (Fig. 4). Several groundwater samples which have high TDS have lower Cl^- concentrations and lie below the trend defined by samples from the pit source. One possible explanation is that the chemical evolution of produced

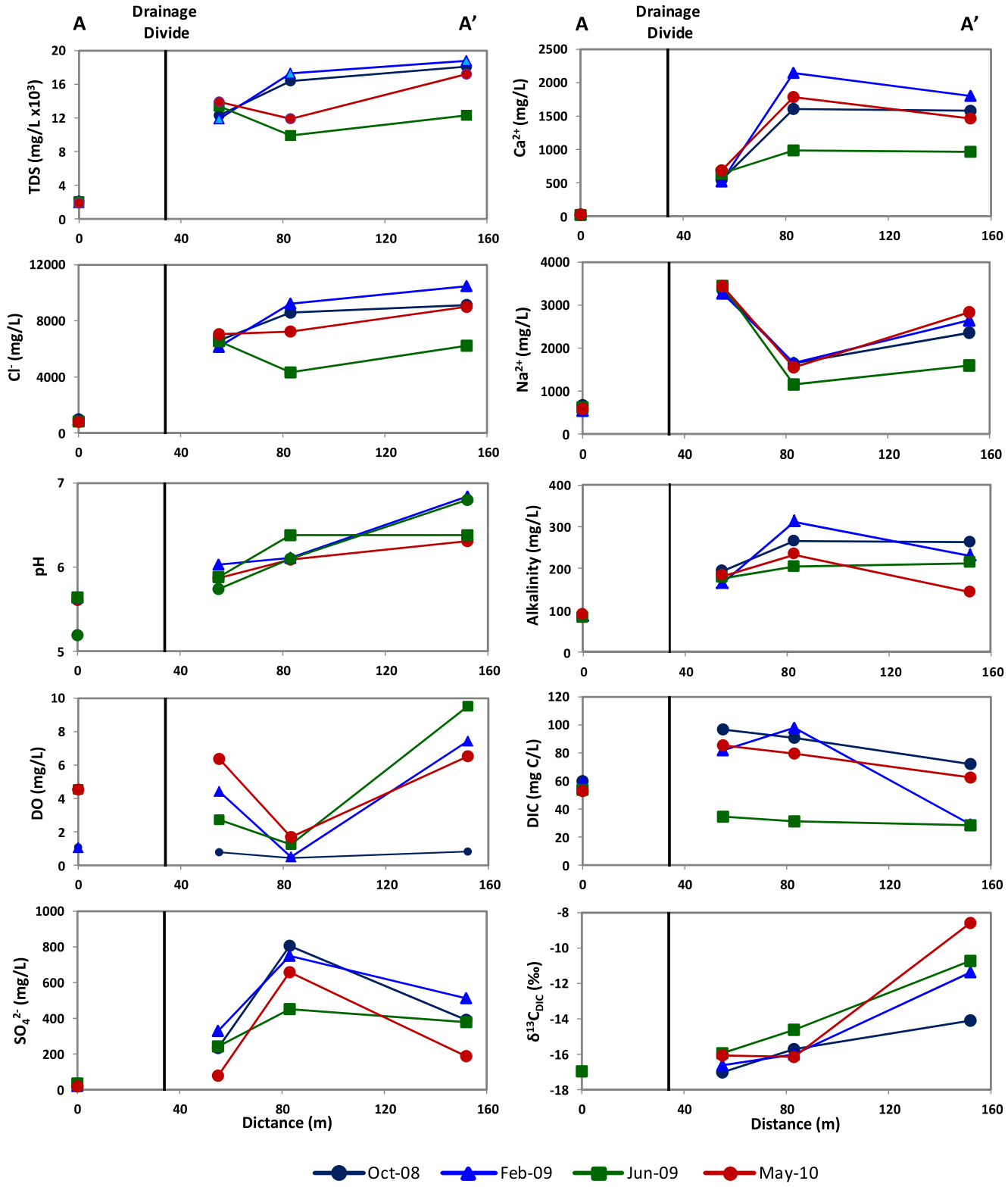

Fig. 3. Spatial variation of total dissolved solids (TDS), Cl^-, pH, dissolved oxygen (DO), Na^+, Ca^{2+}, SO_4^{2-}, alkalinity, dissolved inorganic carbon (DIC) and the stable isotopic composition of DIC ($\delta^{13}C_{DIC}$) along transect A–A′. Vertical lines in the panels represent the position of the drainage divide. Refer to Fig. 1 for transect location.

water brine contaminated fresh groundwater might occur by reverse ion-exchange. Typically, clays prefer cations with a higher charge over cations with low charge (e.g., $Ca^{2+} > Na^+$), but when the lower charged cation exist in much higher concentration compared to a higher charged ion, reverse ion exchange can occur (Hounslow, 1995; Cates et al., 1996; Appelo and Postma, 2005). The relationship between Cl^- vs. Na^+ shown in Fig. 6a reveals that the pit samples (source) lie along the 1:1 Cl^-:Na^+ ratio line. The HCO_3^--rich and SO_4^{2-}-rich water types plot with a Cl^-:Na^+ ratio greater than 1, typical of natural groundwater. In contrast, the Cl^--rich

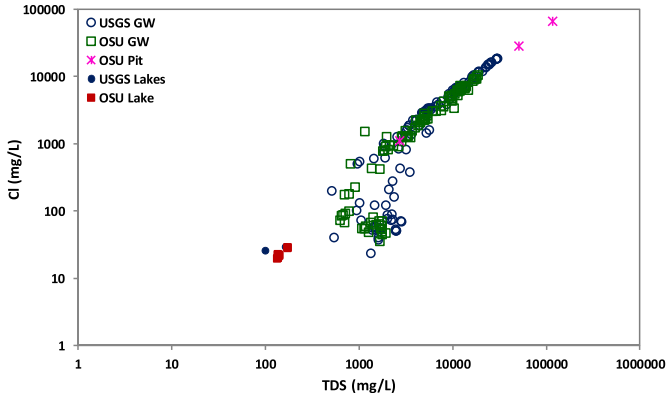

Fig. 4. Scatter plot of the total dissolved solids (TDS) vs. Cl^-. The samples collected by the United States Geological Survey (USGS) were collected between 3/05/2002 and 2/09/2005. Samples collected by Oklahoma State University (OSU) were collected in this study.

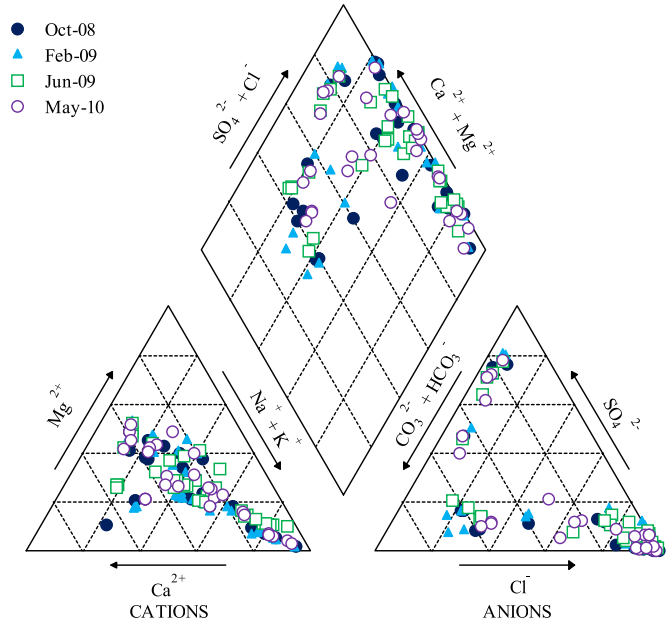

Fig. 5. Piper plot showing the cation and anion proportions for groundwater and lake water at the study site.

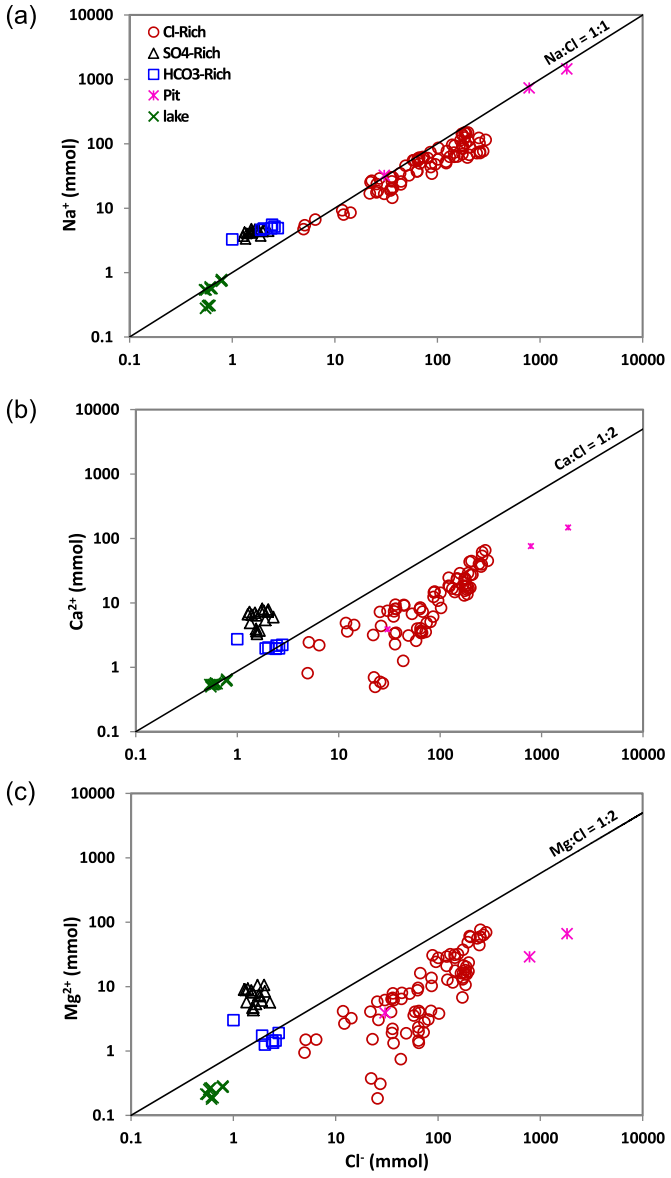

Fig. 6. Scatter plots of (a) Cl^- vs. Na^+, (b) Cl^- vs. Ca^{2+} and (c) Cl^- vs. Mg^{2+}. Groundwaters are identified according to their anion facies.

water type plot slightly below the 1:1 ratio line indicating partial removal of Na^+ perhaps by reverse ion-exchange from groundwater contaminated by produced water brine (Hounslow, 1995; Cates et al., 1996; Drever, 1997; Appelo and Postma, 2005). The relationship between Cl^- vs. Ca^{2+} also shows that the Ca^{2+}:Cl^- ratio in the Cl^--rich water type is lower than the 1:2 ratio for $CaCl_2$ (Fig. 6b) and $MgCl_2$ (Fig. 6c). From the relations between Ca^{2+} and Cl^- and Mg^{2+} and Cl^-, we suggest that reverse ion exchange is likely not a significant source of Ca^{2+} and Mg^{2+}.

5.2.2. Carbonate evolution

The dissolution of carbonates (calcite and dolomite) are a major source of Ca^{2+} and Mg^{2+} which also generate DIC in groundwater.

$$CaCO_3 + H_2O + CO_{2(g)} \leftrightarrow Ca^{2+} + 2HCO_3^- \quad (1)$$

$$CaMg(CO_3)_2 + 2H_2O + 2CO_{2(g)} \leftrightarrow Ca^{2+} + Mg^{2+} + 4HCO_3^- \quad (2)$$

Alkalinity concentrations will increase as calcite and dolomite are weathered by $CO_{2(aq)}$ which should lead to a positive relationship with DIC concentrations (Fig. 7a). There is an overall positive relationship for all groundwater samples. However, the relationship shows significant scatter between alkalinity and DIC, indicating the possibility of multiple processes controlling the carbonate evolution.

In addition to weathering of carbonates that generate DIC, there is likely residual petroleum hydrocarbon that is degraded in the contaminated groundwater by microbes (Godsy et al., 2003) which will add DIC to the groundwater. When Godsy et al. (2003) studied the microbial populations at the study site, they found large populations of aerobic and anaerobic microbes, with the aerobic populations predominating near the surface and iron reducing anaerobic populations predominating downgradient of the contamination source. Interestingly, Godsy et al. (2003) found large populations of sulfate reducing microbial populations, although there were no signs that they were active (low concentrations of

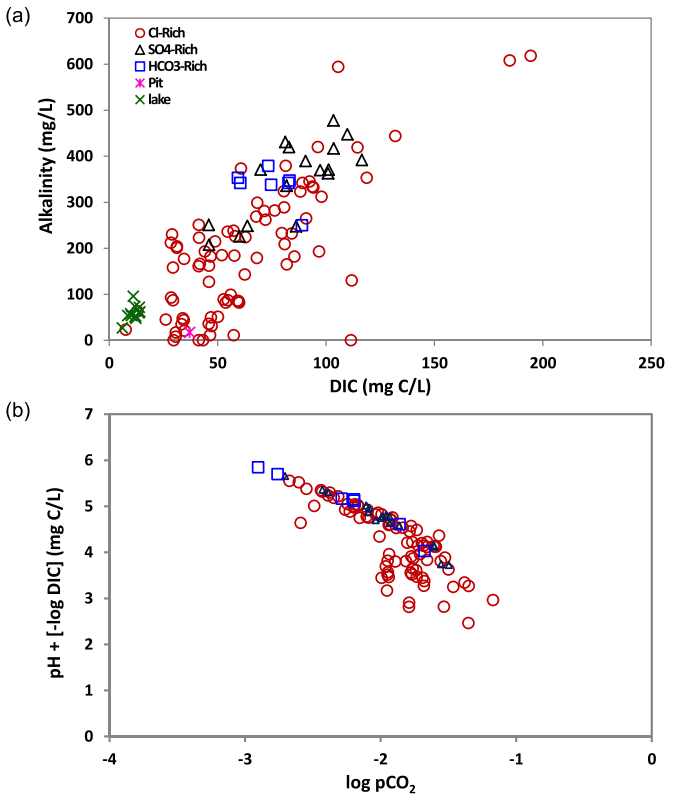

Fig. 7. Scatter plots of (a) dissolved inorganic carbon (DIC) vs. alkalinity and (b) log of the partial pressure of CO_2 ($logpCO_2$) vs. pH + [−logDIC]. Groundwaters are identified according to their anion facies.

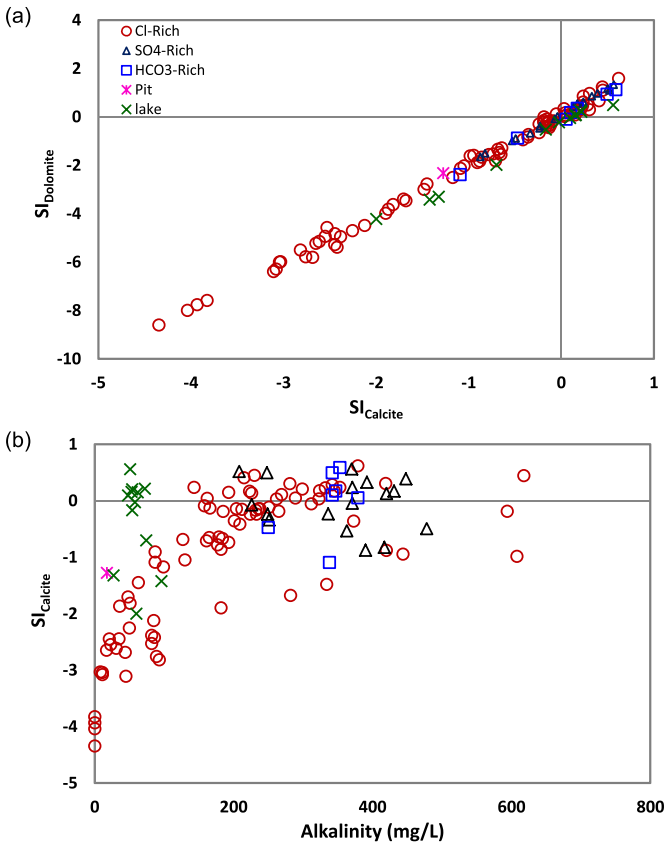

Fig. 8. Scatter plots of (a) saturation indices with respect to (SI)calcite vs. dolomite and (b) alkalinity vs. SIcalcite. Groundwaters are identified according to their anion facies.

S^{2-}) despite high concentrations of SO_4^{2-}. As microbes degrade hydrocarbons, $CO_{2(g)}$ is generated which in addition to the $CO_{2(g)}$ generated from respiration of organic matter in the root zone dissolves and dissociates to produce DIC and/or weather carbonates in the aquifer. Nevertheless, BETEX concentrations were below detection and we suggest that microbial mineralization of hydrocarbons was not an important source of DIC in the contaminated groundwater.

One way to evaluate carbonate weathering and carbonate evolution of groundwater is to use the relationship between pH + [−logDIC] vs. $logpCO_2$ (Fig. 7b). Groundwater samples show a negative relationship with decreasing $logpCO_2$ with increasing pH + [−logDIC] mostly defined by the SO_4^{2-}-rich and HCO_3^--rich groundwater. We suggest that this trend defines groundwater in which there is active dissolution of carbonates which causes increases in pH and DIC concentrations and lowers $logpCO_2$. Although some of the Cl-rich contaminated groundwater also lie along this trend, several samples have lower pH + logDIC (Fig. 7b) suggesting that other processes may be controlling the carbonate evolution of the contaminated groundwater.

It was initially thought that the produced water brine would inhibit the dissolution of calcite and dolomite due to the common ion effect (e.g., Drever, 1997). However, the saturation state of the groundwater, lake water and water from the tar pit with respect to calcite and dolomite are positively correlated and many of the produced water brine contaminated groundwater are significantly undersaturated with respect to calcite and dolomite (Fig. 8a). Also, the positive relationship between alkalinity and the saturation index with respect to calcite is rather poor (Fig. 8b), suggesting that multiple processes may be controlling the carbonate evolution in the groundwater at the study site.

If groundwater in a carbonate aquifer with traces of gypsum is saturated or is near saturation with respect to calcite, dissolution of gypsum may induce dedolomitization (e.g., Back et al., 1983; Bischoff et al., 1994). Dedolomitization generates 1.6 moles of calcite precipitate for every 0.8 mole of dolomite dissolved according to the mass transfer reaction:

$$1.8CaSO_4 + 0.8CaMg(CO_3)_2 \leftrightarrow 1.6CaCO_3 + Ca^{2+} + 0.8Mg^{2+} + 1.8SO_4^{2-} \quad (3)$$

Also, the mass transfer indicates that Ca^{2+} and Mg^{2+} must increase with the increase of SO_4^{2-} at ratios of 1:1.8 and 0.8:1.8, respectively. All water samples at the study site are undersaturated with respect to gypsum (Fig. 9a) indicating the potential for gypsum dissolution. Fig. 9b and c are scatter plots of Ca^{2+} and Mg^{2+} vs. SO_4^{2-}, respectively, along with trend lines showing the Ca^{2+}:SO_4^{2-} and Mg^{2+}:SO_4^{2-} ratios according to reaction (3). The HCO_3^--rich groundwater and SO_4^{2-}-rich groundwater are saturated to near equilibrium with respect to calcite and dolomite (Fig. 8a) and fall along the trend line defined by the expected ratios according to the stoichiometry of dedolomitization (Fig. 9b and c). This suggests that the carbonate evolution in the groundwater at the study site is in part controlled by dedolomitization.

Accordingly, dedolomitization does not appear to be occurring for Cl^--rich groundwater, as many of the samples have Ca^{2+}:SO_4^{2-} ratios that are higher than 1:1.8 and Mg^{2+}:SO_4^{2-} ratios that are higher than 0.8:1.8 and show no correlation between SO_4^{2-} vs. Ca^{2+} or SO_4^{2-} vs. Mg^{2+} (Fig. 9b and c). Relative to the Cl^--rich

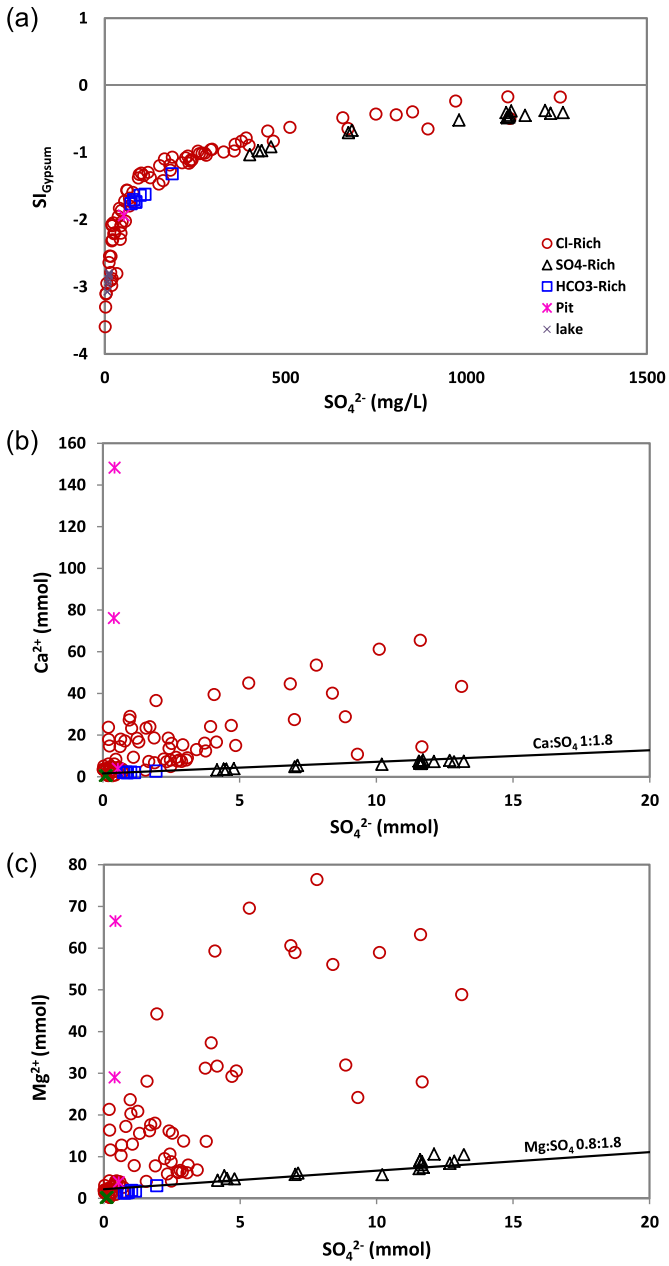

Fig. 9. Scatter plots of (a) SO_4^{2-} vs. the saturation indices for gypsum, (b) SO_4^{2-} vs. Ca^{2+} and (c) SO_4^{2-} vs. Mg^{2+}. Groundwaters are identified according to their anion facies.

groundwater, there are unusually high concentrations of Ca^{2+} in the samples from the tar pit, while the Mg^{2+} concentrations in the water for the tar pit are in the same range as the Cl^--type water samples (Fig. 9b and c). Thus, while dedolomitization can explain the high concentrations of SO_4^{2-} in these samples, dedolomitization is unable to explain the anomalously low Ca^{2+} concentrations relative to samples from the tar pit source.

To explain the anomalously low concentrations of Ca^{2+} in the Cl^--rich groundwaters relative to leachate in the tar pit source (Fig. 9b) we suggest common ion driven calcite precipitation (e.g., Jin et al., 2010):

$$CaSO_4\cdot(2H_2O) + 2HCO_3^- \leftrightarrow CaCO_3 + SO_4^{2-} + 3H_2O + CO_{2(g)} \quad (4)$$

The common ion driven precipitation will reduce the concentrations of Ca^{2+} in the produced water brine contaminated groundwater, and because the common ion driven precipitation does not affect Mg^{2+}, its concentration range will remain similar to that of the source contamination from the tar pit (Fig. 9b and c). This in part may explain the relatively high SO_4^{2-} concentrations in the Cl^--rich groundwater relative to the contaminating source water from the tar pit.

The relatively high concentrations of SO_4^{2-} in groundwater to that of the pit source may result from weathering of pyrite or gypsum which are abundant in the shale unit at this site (Otton et al., 2007). Pyrite can be oxidized by oxygen (e.g., Moses et al., 1987) from oxygen-rich recharge:

$$FeS_2 + 7/2O_2 + H_2O \leftrightarrow Fe^{2+} + 2SO_4^{2-} + 2H^+ \quad (5)$$

In the absence of oxygen, pyrite can be oxidized by nitrates (Kölle et al., 1985):

$$14NO_3^- + 5FeS_2 + 7O_2 + 4H^+ \leftrightarrow 7N_2 + 10SO_4^{2-} + 2Fe^{2+} + 4H^+ \quad (6)$$

The concentrations of Fe > 10 mg/L in anoxic groundwater at produced water brine contaminated sites is due to mobilization of Fe from sediments (Kharaka et al., 2003). Although other reactions can attenuate Fe in the groundwater at this site, the presence of Fe in some locations with anoxic groundwater is likely due to pyrite oxidation. The concentrations of NO_3^- in the aquifer are mostly lower than 3 mg/L (Kharaka et al., 2003). Thus, pyrite oxidation by NO_3^- may in part account for the production of SO_4^{2-}. The protons produced during the pyrite oxidation may further weather the aquifer carbonates as part of the carbonate evolution of groundwater at this site. It is possible that since the groundwater at the site is undersaturated with respect to gypsum (Fig. 9a), natural weathering of gypsum may contribute to the SO_4^{2-} concentrations:

$$H_2O + CaSO_4\cdot 2H_2O \rightarrow Ca^{2+} + SO_4^{2-} + 3H_2O \quad (7)$$

However, gypsum weathering is difficult to determine as many of the groundwater samples do not yield the stoichiometric ratio of Ca^{2+}:SO_4^{2-} of 1:1 expected for such weathering (Fig. 9b) which could be because of the higher Ca^{2+} contributed from the produced water brine.

5.3. Carbon isotopic evolution of groundwater

In natural groundwater, the sources of DIC are (1) the dissolution and dissociation of $CO_{2(g)}$ derived from root respiration and decay of labile soil organic matter in the soil zone and (2) the dissolution of carbonates (Drever, 1997; Appelo and Postma, 2005). In temperate regions, soil $CO_{2(g)}$ that dissolves in groundwater results in a DIC with a $\delta^{13}C_{DIC}$ value of ~−23‰ from microbial degradation of C-3 vegetation (Clark and Fritz, 1997). The dissolved $CO_{2(aq)}$ then weathers aquifer carbonates of marine origin with a $\delta^{13}C$ value of ~0‰ (Clark and Fritz, 1997). In an open system carbonate evolution, the $CO_{2(g)}$ and $CO_{2(aq)}$ remain in equilibrium and the $\delta^{13}C_{DIC}$ increases to approximately −16‰. In contrast, in a closed system carbonate evolution, equal proportions of carbon from $CO_{2(g)}$ and $CaCO_3$ weathering results in $\delta^{13}C_{DIC}$ ~ −11.5‰ (e.g., Clark and Fritz, 1997; Appelo and Postma, 2005).

The DIC concentrations vs. $\delta^{13}C_{DIC}$ for water samples at the study site are shown in Fig. 10a. For all the samples at the study site, there does not appear to be a good relationship between DIC and $\delta^{13}C_{DIC}$, as the increases in the DIC concentration do not necessarily correspond to increases in the $\delta^{13}C_{DIC}$. The $\delta^{13}C_{DIC}$ of the Cl^--rich groundwater shows the widest $\delta^{13}C_{DIC}$ range from −23.5 to −8.6‰,

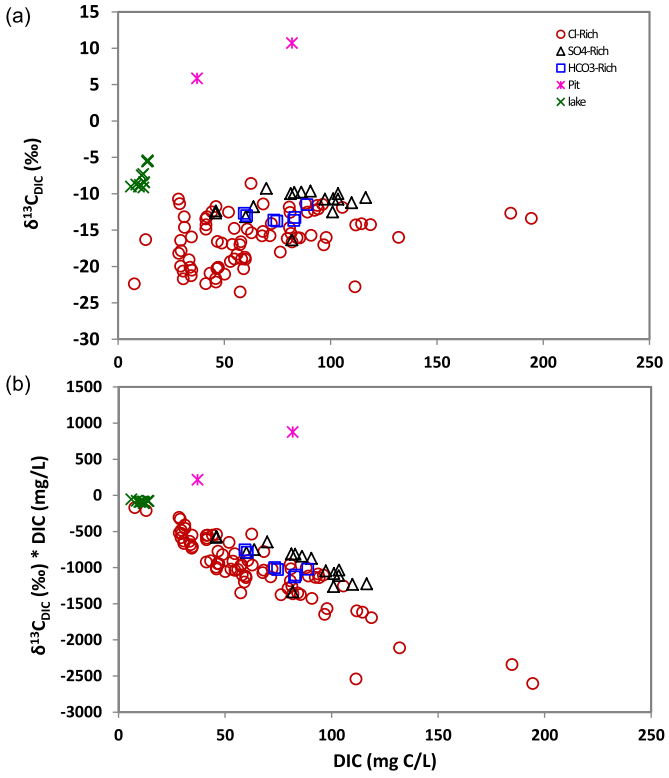

Fig. 10. Scatter plots of (a) stable carbon isotope composition of dissolved inorganic carbon ($\delta^{13}C_{DIC}$) vs. DIC and (b) $\delta^{13}C_{DIC}$*DIC vs. DIC. Groundwaters are identified according to their anion facies.

while in contrast, the range for the SO_4^{2-}-rich groundwater is between −16.3 and −9.2‰ and that for the HCO_3^--rich groundwater is between −13.7 and −11.5‰ (Table S1; Supporting material). Also, the DIC concentration range of 8–194 mg C/L for the Cl^--rich groundwater is wider compared to 46–116 mg C/L for the SO_4^{2-}-rich groundwater and 61–89 mg C/L for the HCO_3^--rich groundwater (Table S1; Supporting material). The variations in the DIC concentrations and the $\delta^{13}C_{DIC}$ for the groundwater at the study site suggest different mechanism for their isotopic evolution. To assess the DIC and $\delta^{13}C_{DIC}$ evolution, we plot the $\delta^{13}C_{DIC}$*DIC vs. DIC (Fig. 10b). The slope of $\delta^{13}C_{DIC}$*DIC vs. DIC is the average $\delta^{13}C_{DIC}$ value of the DIC being added to the groundwater (Hu and Burdige, 2007). The average $\delta^{13}C_{DIC}$ being added to the Cl^--rich groundwater is −12.7‰, while the average $\delta^{13}C_{DIC}$ being added is −9.4‰ for SO_4^{2-}-rich groundwater and −11.6‰ for the HCO_3^--rich groundwater (Table 1).

We suggest that the HCO_3^--rich groundwater with the average $\delta^{13}C_{DIC}$ being added of −11.6‰ is undergoing a closed system DIC evolution from the weathering of marine carbonate by soil zone $CO_{2(g)}$. Appelo and Postma (2005) show that groundwater in some aquifers exhibit $\delta^{13}C_{DIC}$ increases beyond −12‰ with increasing residence time. Explanations for continued $\delta^{13}C_{DIC}$ increases beyond −12‰ are renewed dissolution such as dedolomitization, loss of Ca^{2+} to ion exchange, or bacterial methanogenesis. Methane concentration were not measured in this study, but Godsy et al. (2003) found that methanogenic microorganisms exist in very low population numbers and only trace amounts of CH_4 were detected in groundwater at the study site. We suggest that the $\delta^{13}C_{DIC}$ being added to the SO_4^{2-}-rich water of −9.4‰ is from dedolomitization. Although the average $\delta^{13}C_{DIC}$ being added to the Cl^--rich groundwater of −12.7‰ is much lighter than the expected −11.5‰ for natural DIC evolution in groundwater at the study site, we suggest that the common ion induced calcite precipitation occurring in the Cl^--rich groundwater fractionates the carbon isotopes such that more ^{13}C is partitioned into the precipitate (e.g., Clark and Fritz, 1997) causing the $\delta^{13}C_{DIC}$ in groundwater to be much lighter than expected. Interestingly the Cl^--rich groundwater within the salt scar (Fig. 1) has an average $\delta^{13}C_{DIC}$ value of −16.6‰ indicating that groundwater within the salt scar may be "open" to the soil zone $CO_{2(g)}$ and may be undergoing open system carbonate evolution.

Table 1
Stable carbon isotopic value of the dissolved inorganic carbon (DIC) ($\delta^{13}C_{DIC}$) added to groundwater.

Water sample group	$\delta^{13}C_{DIC\ added}$
Cl^--rich groundwater	−12.7‰
SO_4^{2-}-rich groundwater	−9.4‰
HCO_3^--rich groundwater	−11.6‰
Lake samples	−2.6‰
Pit samples	14.7‰

6. Conclusions

We investigated the carbonate evolution of fresh groundwater contaminated by produced water brine with hydrocarbon from more than 60 y of petroleum production. The produced water brine was stored in unlined earthen pits and eventually seeped into the fresh groundwater aquifer creating a high salinity contaminant plume. The groundwater at the site could be best characterized by anion facies. The anion facies were HCO_3^--rich, SO_4^{2-}-rich and Cl^--rich, which suggest that the chemical evolution of groundwater at the site was controlled by multiple processes. The HCO_3^--rich groundwater was produced from dissolution of aquifer carbonates by $CO_{2(g)}$ from the soil zone. The SO_4^{2-}-rich groundwater was produced from gypsum induced dedolomitization. The Cl^--rich groundwater resulted from produced water brine contamination and the groundwater undergoes common ion induced calcite precipitation.

The DIC and $\delta^{13}C_{DIC}$ in the different types of groundwater undergo different carbonate evolution and can be described by the average $\delta^{13}C_{DIC}$ added to the groundwater DIC pool. The average $\delta^{13}C_{DIC}$ added to the HCO_3^--rich groundwater was −11.6‰, −9.4‰ for the SO_4^{2-}-rich groundwater and −12.7‰ for the Cl^--rich groundwater. The $\delta^{13}C_{DIC}$ in the HCO_3^--rich groundwater ranged between −13.0 and −11.5‰ and the DIC is from a closed system carbonate evolution from soil $CO_{2(g)}$ and carbonate. The $\delta^{13}C_{DIC}$ in the SO_4^{2-}-rich groundwater ranged between −16.3 and −8.6‰. Gypsum induced dedolomitization in the SO_4^{2-}-rich groundwater was responsible for the increase in the $\delta^{13}C_{DIC}$ beyond the −11.5‰ observed for HCO_3^--rich groundwater. The $\delta^{13}C_{DIC}$ in the Cl^--rich groundwater ranged between −23.5 and −8.6‰. Although the range in the $\delta^{13}C_{DIC}$ is very wide for the Cl^--rich groundwater, DIC evolution is dominated by common ion induced calcite precipitation which removes heavy ^{13}C from the DIC pool. The results of this study show that fresh water aquifer contaminated by produced water alters the carbonate evolution which is traceable from the behavior of the major ions and DIC and the $\delta^{13}C_{DIC}$.

Acknowledgments

This research was partially supported by a graduate student research grant from the Geological Society of America to EJS. We thank M. Abbott of the Osage-Skiatook Petroleum Environmental Research project for arranging access to the study site and for providing information and data about the site. We thank C. Geyer, N. Paizis, E. Akoko, L. Guidry, J. Majors and T. Troiani for field and/or laboratory assistance. This is Oklahoma State University Boone

Pickens School of Geology contribution number 2015-26.

Appendix A. Supplementary data

Supplementary data related to this article can be found at http://dx.doi.org/10.1016/j.apgeochem.2015.08.001.

References

Appelo, C.A.J., Postma, D., 2005. Geochemistry, Groundwater and Pollution. CRC Press.

Atekwana, E.A., Atekwana, E., Legall, F.D., Krishnamurthy, R.V., 2005. Biodegradation and mineral weathering controls on bulk electrical conductivity in a shallow hydrocarbon contaminated aquifer. J. Contam. Hydrol. 80 (3), 149–167.

Atekwana, E.A., Krishnamurthy, R.V., 1998. Seasonal variations of dissolved inorganic carbon and $\delta^{13}C$ of surface waters: application of a modified gas evolution technique. J. Hydrol. 205 (3), 265–278.

Back, W., Hanshaw, B.B., Plummer, L.N., Rahn, P.H., Rightmire, C.T., Rubin, M., 1983. Process and rate of dedolomitization: mass transfer and ^{14}C dating in a regional carbonate aquifer. Geol. Soc. Am. Bull. 94 (12), 1415–1429.

Bischoff, J.L., Juliá, R., Shanks, W.C., Rosenbauer, R.J., 1994. Karstification without carbonic acid: bedrock dissolution by gypsum-driven dedolomitization. Geology 22 (11), 995–998.

Cates, D.A., Knox, R.C., Sabatini, D.A., 1996. The impact of ion exchange processes on subsurface brine transport as observed on piper diagrams. Ground Water 34 (3), 532–544.

Calmbach, L., 1997. AquaChem Computer Code-version 3.7. 42. Waterloo, Ontario, Canada, N2L 3L3.

Clark, I.D., Fritz, P., 1997. Environmental Isotopes in Hydrogeology. CRC Press.

Currell, M.J., Cartwright, I., 2011. Major-ion chemistry, $\delta^{13}C$ and $^{87}Sr/^{86}Sr$ as indicators of hydrochemical evolution and sources of salinity in groundwater in the Yuncheng Basin, China. Hydrogeol. J. 19 (4), 835–850.

Drever, J.I., 1997. The Geochemistry of Natural Waters: Surface and Groundwater Environments. Prentice-Hall.

Fang, J., Barcelona, M.J., Krishnamurthy, R., Atekwana, E., 2000. Stable carbon isotope biogeochemistry of a shallow sand aquifer contaminated with fuel hydrocarbons. Appl. Geochem. 15 (2), 157–169.

Gardner, W.E., 1957. Geology of the Barnsdall Area, Osage County, Oklahoma (Master's thesis). The University of Oklahoma, Norman, Oklahoma.

Godsy, E.M., Hostettler, F.D., Warren, E., Paganelli, V.V., Kharaka, Y.K., 2003. Environmental Impacts of Petroleum Production: the Fate of Petroleum and Other Organics Associated with Produced Water from the Osage-Skiatook Petroleum Environmental Research Sites, Osage County, Oklahoma. U.S. Geological Survey Water-Resources Investigations Report 03-4260.

Hach Company, 1992. Water Analysis Handbook. Hach Company, Loveland, Co.

Herkelrath, W.N., Kharaka, Y.K., Thordsen, J.J., Abbott, M.M., 2007. Hydrology and subsurface transport of oil-field brine at the U.S. Geological Survey OSPER site "A", Osage County, Oklahoma. Appl. Geochem. 22 (10), 2155–2163.

Hounslow, A., 1995. Water Quality Data: Analysis and Interpretation. CRC Press.

Hu, X., Burdige, D.J., 2007. Enriched stable carbon isotopes in the pore waters of carbonate sediments dominated by seagrasses: evidence for coupled carbonate dissolution and reprecipitation. Geochim. Cosmochim. Acta 71 (1), 129–144.

Jin, L., Siegel, D.I., Lautz, L.K., Mitchell, M.J., Dahms, D.E., Mayer, B., 2010. Calcite precipitation driven by the common ion effect during groundwater–surface-water mixing: a potentially common process in streams with geologic settings containing gypsum. Geol. Soc. Am. Bull. 122 (7–8), 1027–1038.

Kharaka, Y.K., Kakouros, E., Thordsen, J.J., Ambats, G., Abbott, M.M., 2007. Fate and groundwater impacts of produced water releases at OSPER "B" site, Osage County, Oklahoma. Appl. Geochem. 22 (10), 2164–2176.

Kharaka, Y.K., Otton, J.K., 2003. Environmental Impacts of Petroleum Production: Initial Results from the Osage-Skiatook Petroleum Environmental Research Sites, Osage County, Oklahoma. US Department of the Interior, US Geological Survey.

Kharaka, Y.K., Thordsen, J.J., Kakouros, E., Abbott, M.M., 2003. Environmental Impacts of Petroleum Production: Fate of Inorganic and Organic Chemicals in Produced Water from the Osage-Skiatook Petroleum Environmental Research Sites, Osage County, Oklahoma. U.S. Geological Survey Water-Resource Investigation Report 03-4260.

Kharaka, Y.K., Otton, J.K., 2007. Environmental issues related to oil and gas exploration and production-preface. Appl. Geochem. 22 (10), 2095–2098.

Kharaka, Y.K., Thordsen, J.J., Kakouros, E., Herkelrath, W.N., 2005. Impacts of petroleum production on ground and surface waters: results from the Osage–Skiatook Petroleum Environmental Research A site, Osage County, Oklahoma. Environ. Geosci. 12 (2), 127–138.

Kölle, W., Strebel, O., Böttcher, J., 1985. Formation of sulfate by microbial denitrification in a reducing aquifer. Water Supply 3 (1), 35–40.

Moses, C.O., Nordstrom, D.K., Herman, J.S., Mills, A.L., 1987. Aqueous pyrite oxidation by dissolved oxygen and by ferric iron. Geochim. Cosmochim. Acta 51 (6), 1561–1571.

Nicholson, C.A., Fathepure, B.Z., 2005. Aerobic biodegradation of benzene and toluene under hypersaline conditions at the Great Salt Plains, Oklahoma. FEMS Microbiol. Lett. 245 (2), 257–262.

Otton, J.K., Zielinski, R.A., Smith, B.D., Abbott, M.M., 2007. Geologic controls on movement of produced-water releases at US Geological Survey Research Site A, Skiatook lake, Osage county, Oklahoma. Appl. Geochem. 22 (10), 2138–2154.

Parker, S.R., Gammons, C.H., Smith, M.G., Poulson, S.R., 2012. Behavior of stable isotopes of dissolved oxygen, dissolved inorganic carbon and nitrate in groundwater at a former wood treatment facility containing hydrocarbon contamination. Appl. Geochem. 27 (6), 1101–1110.

Parkhurst, D.L., Appelo, C., 1999. User's Guide to PHREEQC (Version 2): a Computer Program for Speciation, Batch-reaction, One-dimensional Transport, and Inverse Geochemical Calculations, p. 312. US Geological Survey Water-Resources Investigations Report 99-4259.

Scow, K.M., Hicks, K.A., 2005. Natural attenuation and enhanced bioremediation of organic contaminants in groundwater. Curr. Opin. Biotechnol. 16 (3), 246–253.

Su, X.S., Lv, H., Zhang, W.J., Zhang, Y.L., Jiao, X., 2013. Evaluation of petroleum hydrocarbon biodegradation in shallow groundwater by hydrogeochemical indicators and C, S-isotopes. Environ. Earth Sci. 69 (6), 2091–2101.

Ulrich, A.C., et al., 2009. Effect of salt on aerobic biodegradation of petroleum hydrocarbons in contaminated groundwater. Biodegradation 20 (1), 27–38.

Whittemore, D.O., 2007. Fate and identification of oil-brine contamination in different hydrogeologic settings. Appl. Geochem. 22 (10), 2099–2114.